

Optical parametric sources for the infrared/Sources optiques paramétriques pour l'infrarouge

## Specific architectures for optical parametric oscillators

Antoine Berrou, Jean-Michel Melkonian, Myriam Raybaut, Antoine Godard,  
Emmanuel Rosencher, Michel Lefebvre\*

ONERA – Office national d'études et de recherches aérospatiales, B.P. 72, 92322 Châtillon cedex, France

Available online 26 October 2007

---

### Abstract

Optical parametric oscillators are coherent light sources showing properties that are not encountered with usual laser sources. This article deals with optical architectures that take advantage of the specific properties of the three-wave mixing parametric interaction. We show that optical cavities can be specifically designed to increase either the optical conversion of the parametric process or to reduce dramatically the emitted line width. *To cite this article: A. Berrou et al., C. R. Physique 8 (2007).*

© 2007 Académie des sciences. Published by Elsevier Masson SAS. All rights reserved.

### Résumé

**Architectures spécifiques aux oscillateurs paramétriques optiques.** Les oscillateurs paramétriques optiques sont des sources de lumière cohérente qui présentent des propriétés que l'on ne rencontre pas avec les sources laser usuelles. Cet article traite d'architectures optiques qui tirent avantage des propriétés spécifiques du processus de mélange paramétrique à trois ondes. Nous montrons que des cavités optiques peuvent être spécifiquement conçues pour augmenter le rendement de conversion optique ou pour réduire fortement la largeur de raie produite. *Pour citer cet article : A. Berrou et al., C. R. Physique 8 (2007).*

© 2007 Académie des sciences. Published by Elsevier Masson SAS. All rights reserved.

*Keywords:* Optical parametric oscillator; Specific optical cavity; Mid-IR tuneable source

*Mots-clés :* Oscillateur paramétrique optique ; Cavité optique spécifique ; Source IR moyen accordable

---

### 1. Introduction

Optical parametric oscillators (OPOs) are very attractive devices to generate coherent light in spectral domains that are not covered by lasers. At first glance, OPO devices seem to be very close to optically pumped lasers given that they are designed from the combination of an optical cavity containing an amplification medium (the nonlinear crystal) and an external optical source (the pump laser). However, OPOs have specific properties that lead us to design original coherent light sources capable of meeting technical requirements for new applications. Among the specificities of parametric sources, one can notice that the parametric conversion is an instantaneous gain process that it is sustained without any storage of the pump energy. In addition, the parametric conversion involves a nonlinear interaction between three waves where the relative phase between the three fields plays a major role. In the following

---

\* Corresponding author.

*E-mail address:* [michel.lefebvre@onera.fr](mailto:michel.lefebvre@onera.fr) (M. Lefebvre).

sections, we give some examples of specific OPO architectures, which have been developed at ONERA either to improve the conversion efficiency of the parametric process or to produce a narrow line width tuneable radiation.

## 2. Improvement of the optical conversion efficiency

### 2.1. OPO–OPA architecture

Most OPO configurations use only one of the two radiations that are produced from the downconversion of the input pump laser beam. The maximum optical yield is so limited to the quantum defect that relies on the difference of the two wavelengths. Thus, the conversion efficiency becomes particularly low if one aims to produce mid-IR radiation such as 5  $\mu\text{m}$  from a well mature 1  $\mu\text{m}$  laser; in that case, the maximum conversion efficiency is only 20%. This leads us to develop more efficient configurations where the unused wavelength acts as a pump radiation in a second interaction. Such an approach is particularly promising when both the first and second nonlinear interactions contribute to the production of a radiation at the same final wavelength, as it is schemed in Fig. 1(b). In this situation, called OPO–OPA (Optical Parametric Oscillator – Optical Parametric Amplifier), one idler photon is produced from the initial pump laser photon while a second idler photon is obtained at the same wavelength from the downconversion of the signal photon coming from the first interaction. Thus, the maximum optical yield (pump  $\rightarrow$  idler) reaches two times the quantum defect.

The OPO–OPA approach was first proposed by Koch et al. [1], who predicted an idler photon conversion efficiency better than 100% over a large dynamic range of pump power, for a proper choice of the nonlinear coupling parameters between the OPO and OPA interactions. Yet, it remains to be proved that the OPO–OPA approach is well suited to design a high-energy mid-IR source. Clearly, the nanosecond time scale is well suited to produce high-energy pulses and indeed, we have to consider the influence of the parametric radiation build-up time on the expected conversion efficiency. In addition, nonlinear crystals with a large optical aperture have to be implemented at high energy pump levels with the detrimental effect that bulk crystals (KTP, LiNbO<sub>3</sub>, ...) suffer from rather low nonlinear coefficients compared to periodically quasi-phase matched materials.

Recently, our group has investigated both theoretically and experimentally the potentialities of the OPO–OPA configuration in the nanosecond regime. From the theoretical analysis, it was concluded that the conversion efficiency of the OPO–OPA approach shows less saturation compared to a classical singly resonant OPO. Such a behaviour results from the fact that the nonlinear gain experienced by the resonating field in the cavity is balanced by the nonlinear loss in the OPA stage. Thus, the OPO–OPA configuration overtakes the singly resonant OPO at a high pumping level, typically two times above the threshold of oscillation. The experimental work was conducted with two bulk KTA crystals inserted within a flat–flat resonator. The two mirrors have a maximum reflection at the signal wavelength (1.54  $\mu\text{m}$ ) produced from the OPO stage, see Fig. 2. The pump beam at 1.06  $\mu\text{m}$  is delivered by a Nd:YAG laser running at 12.5 Hz, the maximum energy is 90 mJ in 27 ns long pulses. The idler and signal radiations coming respectively from the OPO and the OPA, are produced at 3.45  $\mu\text{m}$ . Given that the OPA is pumped by the 1.54  $\mu\text{m}$  radiation, one finds that the OPA idler wave stands around 2.78  $\mu\text{m}$ . Thus, at the exit of the OPO–OPA architecture depicted in Fig. 2, one obtains the following radiations:

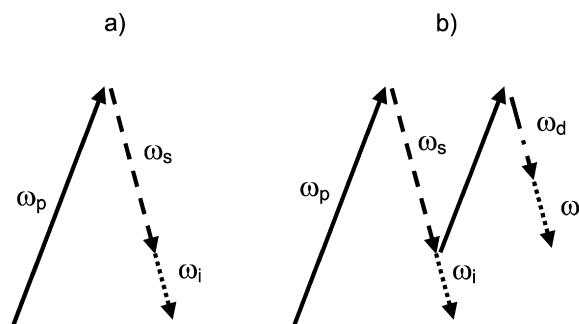


Fig. 1. (a) OPO frequency diagram; (b) OPO–OPA frequency diagram.

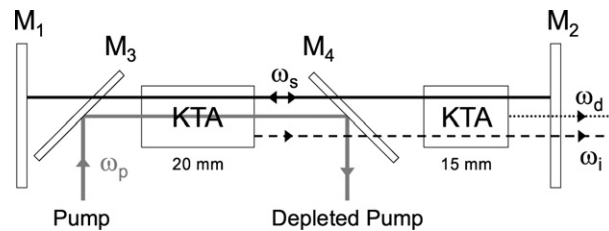


Fig. 2. Scheme of the OPO-OPA experimental arrangement.

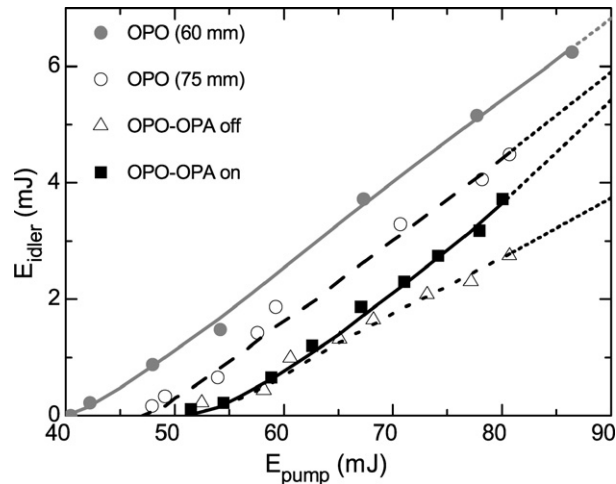


Fig. 3. Experimental dependence of the output idler energy versus input pump energy; results have been obtained for a singly resonant OPO with a 60 mm or 75 mm-long cavity and for the OPO-OPA approach with and without the parametric amplification.

- one part of the 1.54  $\mu\text{m}$  signal beam produced from the OPO;
- the 3.45  $\mu\text{m}$  wavelength produced both in the OPO and in the OPA;
- the 2.78  $\mu\text{m}$  wavelength corresponding to the signal field produced in the OPA.

We notice that two radiations are simultaneously produced around 3  $\mu\text{m}$ ; this feature is well suited for broadband applications such as laser ultrasonic inspection of composite materials where high-energy pulses (several tens of mJ) in the 3  $\mu\text{m}$  spectral range are needed [2].

In order to quantify the OPO-OPA potentialities, three situations have been compared:

- a singly resonant OPO with a short cavity (60 mm);
- a singly resonant OPO with a cavity length of 75 mm corresponding to the length of the OPO-OPA cavity;
- the OPO-OPA geometry reported in Fig. 2, where a 15-mm-long KTA crystal has been inserted within the cavity for amplification at 3.45  $\mu\text{m}$ ; the crystal length has been chosen for optimizing the conversion efficiency. The KTA crystal is used in Type-II phase matching with  $\varphi = 70^\circ$  and  $\theta = 0^\circ$ , the end faces are antireflection coated at the signal and idler wavelengths. Nevertheless, one measures a transmission loss of 16% at the idler wavelength due to an optical absorption within the two coatings.

Fig. 3 shows the output idler energy as a function of the incident pump energy for these three different configurations. The short-cavity OPO displays an oscillation threshold of 40 mJ and an efficiency of 7.2% at a pump energy of 86.4 mJ. As concerns the 75 mm-long singly resonant OPO, one finds the same slope efficiency whereas the threshold increases to 48 mJ. Indeed, during the same amount of time, the generated idler and signal waves perform fewer round trips in the long cavity than in the short one. Hence these two fields experience less amplification and need more time to build up from the noise. Because of the limited duration of the pump pulses, this build-up time reduces the efficiency of the long-cavity OPO efficiency and increases its threshold. The OPO-OPA exhibits a threshold of 50 mJ whether

the OPA process is phase-matched (OPA on) or not (OPA off). The rise of the threshold is related to the increase of the optical cavity length when the second crystal is inserted. However, the frequency conversion in the second crystal does not affect the OPO threshold, because it is not effective until the signal builds up in the cavity. When the OPA is off, the OPO produces 2.7 mJ of idler energy for a pump of 81 mJ, associated to 3.3% of energy efficiency. When the OPA is on, the OPO generates 3.8 mJ and 4.7% efficiency for the same pump power. Thus, we obtain a 35% increase of the idler energy at the maximum available pump energy when the OPA process is phase-matched. It is important to note, however, that the OPO–OPA performance is strongly lowered by the unwanted absorption in the coatings of the second KTA crystal.

From this experimental work, one concludes that the OPO–OPA does not deliver more idler energy at 3.45  $\mu\text{m}$  than a single-crystal OPO for moderate pump energies, i.e. less than 2 times above threshold, despite the 40% energy increase brought by the OPA process. This result clearly evidences the importance of cavity lengthening. Nevertheless, a very interesting feature of the OPO–OPA relies on the production of an additional wavelength, according to the difference frequency process  $1.54\text{--}3.45\ \mu\text{m} \rightarrow 2.78\ \mu\text{m}$ . This extra radiation also leads to an enhancement of the mid-IR output and makes the OPO–OPA an interesting device for applications that require an intense broadband mid-IR emission.

## 2.2. Cross-resonant OPO

In singly resonant OPOs, one wave oscillates within an optical cavity whereas the other one is out coupled at each round trip. In such a configuration, the signal and idler radiations play an asymmetric role in the energy transfer process: on the one hand, the driving force in the parametric interaction is enhanced by the presence of the resonant field which plays a catalytic role in the parametric process; on the other hand, the nonresonant wave, which is completely out coupled after the nonlinear conversion, acts as a nonlinear loss for the parametric amplification. The idea of the cross-resonant OPO is to eliminate this asymmetric role by using a cavity where the two radiations contribute equivalently to the parametric conversion process. As depicted in Fig. 4(a), this can be achieved with a four-mirror cavity containing two crystals. The coatings of the four mirrors are carefully designed so that the pump beam passes through the two crystals while the signal and idler waves are out coupled after the first and second crystal, respectively.

In cross-resonant OPOs, the signal and idler fields have a specific axial distribution. Indeed, the two fields are jointly resonant but they grow in different longitudinal parts of the cavities. To sustain this mixed oscillation, the generated idler power, which is reached at the end of the first crystal must lead to a value of the nonlinear gain in the second crystal that yields a generated signal power such that the signal power at the first crystal entrance is stationary, see Fig. 4(b). Due to the mixed oscillation at the signal and idler wavelengths, the first interpretation was to consider that the cavity does not impose any resonance condition so, it was concluded that a cross-resonant OPO is just an optical generator [3]. Yet, a more detailed analysis of the three-wave interaction demonstrates that the mixed oscillation can only takes place at discrete frequencies that are imposed by the total length of the four-mirror cavities. Basically, we should bear in mind that the parametric process is based on a coherent interaction that imposes the relative phase between the three connecting fields. Thus, even if the two waves are alternatively out coupled through M2 and M4, the phase is not lost in a round trip and consequently the oscillation frequencies are distributed, as usual, along a discrete

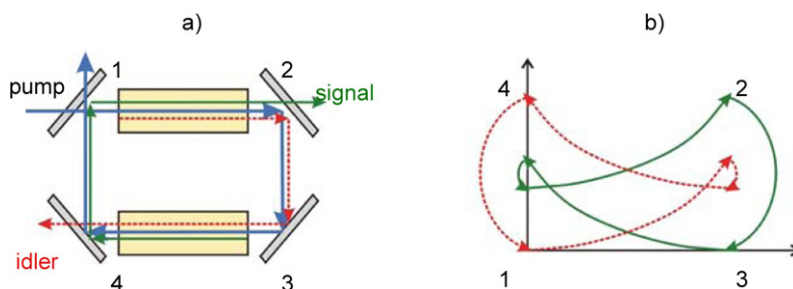


Fig. 4. (a) Cross-resonant OPO geometry and (b) spatial evolution of the signal and idler power along one round-trip.

longitudinal mode comb. Considering that the phase shift accumulated at each round trip must be a multiple integer of  $2\pi$ , one readily demonstrated [4], that the intermode spacing ( $\Delta\omega$ ) is given by:

$$\Delta\omega = \frac{2\pi c}{(n_s + n_i)L + 2L'} \quad (1)$$

where  $c$  is the speed of light,  $n_s$  and  $n_i$  are the indexes of refraction at the signal and idler wavelengths, respectively,  $L$  is the crystal length and  $L'$  is the cavity length outside the two crystals. Given the intermode spacing value, one concludes that the cross-resonant OPO cavity is equivalent to a ring cavity with an optical length  $L_{\text{cav}}$  defined by  $L_s = (n_s + n_i)L + 2L'$ .

Another specific property of a cross-resonant OPO is its low sensitivity to back conversion, by comparison with singly or doubly resonant OPOs. Indeed, singly and doubly resonant OPOs suffer from the back conversion process (signal + idler  $\rightarrow$  pump) that has two major drawbacks at high pumping levels: the saturation of the optical conversion efficiency and the degradation of the beam quality. Cross-resonant OPOs are less sensitive to the back conversion process given that neither the signal nor the idler are stored within the optical cavity. Fig. 5 illustrates such a behaviour under continuous wave (cw) pumping. The plotted curves have been calculated from a rate equation formalism, detailed in [4] and [5]. The optical conversion efficiency has been determined for two situations: a cross-resonant OPO and a singly resonant OPO with a 50% output coupler for the resonant wave so as to ensure the same threshold of oscillation in both cases. From Fig. 5, it is seen that the saturation of the output at high pumping levels is stronger for the singly resonant OPO than for the cross-resonant OPO. The theoretical 100% pump depletion occurs at  $X = 2.4$  for the singly resonant OPO and at  $X = 3.5$  for the cross-resonant OPO. Furthermore, the efficient depletion range is much larger for the cross-resonant OPO than for the singly resonant case. This effect is due to a stronger pump reconversion in the singly resonant configuration as a result of the high intracavity power at the oscillating wavelength.

Finally, one has to emphasize that the cross-resonant OPO is an attractive geometry to go further in the infrared domain through a difference frequency process. Indeed, as depicted in Fig. 6, this geometry delivers two radiations in two distinct directions so one can adjust separately the two beam properties (polarization, diameter, direction) and thus the efficiency of the difference frequency process. In order to demonstrate the potentiality to produce longer wavelengths, the signal and idler radiations were mixed in a 48-mm long AR-coated CdSe crystal, see Fig. 6. As it

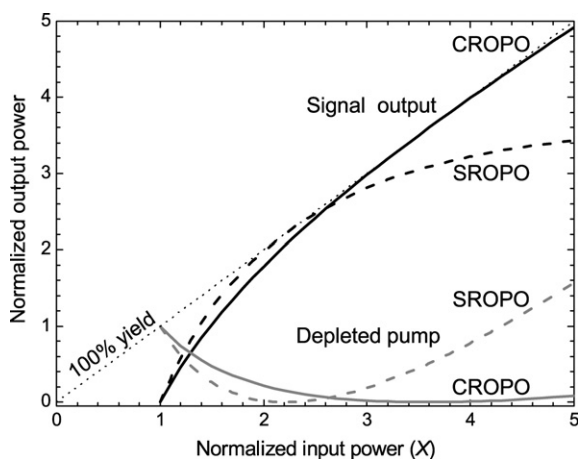


Fig. 5. Calculated dependence of the signal output power and depleted pump power versus the input pump power. Calculations have been carried out for a singly resonant OPO with a 50% output coupler at the signal wavelength and for the cross-resonant OPO. The input power ( $X$ ) is normalized at the threshold of oscillation value.

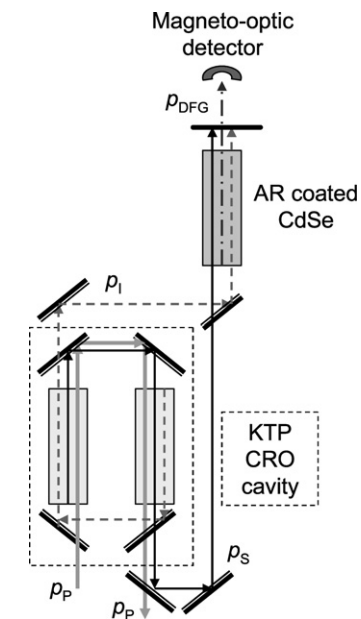


Fig. 6. Experimental set-up for the production of a  $12\ \mu\text{m}$  radiation from the frequency mixing of the signal and idler radiations coming from the cross-resonant OPO.

is well known, CdSe is a semiconductor material, which is well appropriate for mid-IR generation thanks to its wide transparency-range up to 22  $\mu\text{m}$  and its high second order nonlinear coefficient  $d_{31}$  (18 pm/V). In this experiment, the signal and idler waves at 1970 and 2340 nm respectively, were mixed to generate a 12  $\mu\text{m}$  radiation. Since the two KTP cross-resonant OPO operated in type II phase matching, the polarizations of the emitted waves were adapted for type II phase matching in CdSe. Otherwise, each polarization could be independently adjusted by inserting a half-wave plate prior to the beam recombination. To avoid damage of the CdSe crystal coatings, we limited the total incident energy to 1 mJ. In this configuration, the two 500  $\mu\text{J}$  beams were mixed in the CdSe crystal and we maximize the output energy by optimizing the two beams overlap as well as the CdSe crystal orientation. The maximum 12  $\mu\text{m}$  energy that we achieved, was about 25  $\mu\text{J}$  yielding to an energy conversion efficiency of 2.5%. Such a value is excellent for a difference frequency process involving input pulses of a few nanoseconds time-scale and considering the quantum defect ( $\approx 6$ ) between the incoming and generated waves. It was obtained thanks to the cross-resonant device that provides intrinsically the optimal conditions for the mixing process i.e. two pulses of similar energy and spatiotemporal shapes.

### 3. Reduction of the spectral line width

There is a considerable interest in narrow line width widely tunable laser sources, motivated by the emergence of new topics such as quantitative analysis of trace gases in the atmosphere, environmental monitoring, medical diagnostic, coherent laser radar, . . . For such applications, one needs a laser source delivering a narrow line width radiation in order to address a specific line of molecular or atomic species. In addition, the frequency of the optical source has to be tuneable over the mid-IR domain where most of species of interest show strong absorption lines. Clearly, nanosecond OPOs provide the required wavelength tuneability but they do not deliver the narrow line width emission when they are implemented in their basic singly resonant configuration. Thus, various methods have been studied and proposed to achieve single-frequency output. Before dealing with the doubly resonant approach that has been mainly developed at ONERA, we give below a short review of previous works.

#### 3.1. State of the art

Following previous approaches devoted to broadband lasers such as dye or titanium sapphire lasers, one strategy consists in the introduction of selective elements, i.e. Fabry Perot étalons, dispersive prisms or gratings inside the cavity. In such a way, L.B. Kreuzer [6] demonstrated in 1969 that single-longitudinal-mode oscillation can be achieved from a nanosecond singly resonant OPO if a Fabry Perot étalon is inserted within the optical cavity. In this pioneering work, the side mode suppression ratio (SMSR) was better than 10 dB. However, the method did not received a great attention and only a few works have been done so far given that this technique suffers from several drawbacks:

- the insertion losses appear as a main limitation regarding the low gain value that is obtained in parametric processes;
- if small beam sizes are used, the threshold of oscillation rapidly increases when the étalon is tilted for frequency tuning;
- in case of a wide parametric gain band width (type 0 or type I phase matching close to degeneracy), two étalons have to be used [7], increasing so the complexity and subsequently the oscillation threshold;
- the cavity has to be as short as possible to well separate the axial modes of the cavity so that the étalon can select only one longitudinal mode;
- a high finesse étalon with a high damage threshold has to be used to support the pump beam intensity;
- tuning the output wavelength needs to adjust in synchronism the étalon angle and the length of the cavity.

An alternative approach relies on dispersive cavities that have been mainly implemented in OPOs under the well-known Littman configuration. Although this arrangement was fully validated with dye lasers, previous configurations cannot be readily duplicated to OPOs given the specific properties of the parametric conversion. More precisely, the relatively low reflectivity of a diffraction grating is a serious limitation pertaining to the low amplification coefficient sustained in OPOs, compared to dye lasers. Thus, efficient nonlinear crystals such as PPKTP [8] and PPLN [9] have been selected for OPOs working in the Littman configuration. The grating is usually inserted at grazing-incidence

to introduce sufficient dispersion for single-mode operation even close to degeneracy. Under such conditions, the spectral line width of the OPO stands around 200 MHz with 10 ns pulse duration. Nonetheless, the pumping level has to be maintained close to the threshold of oscillation (1.5 above threshold, typically) to avoid optical damage, so limiting the parametric conversion efficiency. Although best performances have been obtained with type 0 periodically poled materials thanks to their high nonlinearity, operation under type II phase matching remains very attractive to achieve stable single mode output given the narrow parametric gain band width. The lower efficiency obtained in type II phase matching can be compensated by using a double-pass pump geometry with one [10] or two nonlinear crystals [11]. Compared to OPOs with intracavity étalons, Littman OPO cavities provide a larger continuous single-mode scanning range. Still, the additional losses introduced by the grating at grazing incidence, as well as the increase of the cavity length, mean that the threshold of oscillation is difficult to achieve without any optical damage.

To overcome the detrimental effect of insertion losses, architectures based on injection seeding techniques have also been tested. In 1969, J.E. Bjorkholm et al. [12] carried out the first demonstration of frequency locking by seeding a LiNbO<sub>3</sub> singly resonant OPO with a cw radiation. Next, the method has been tested with various seed sources. Basically, the OPO oscillation is forced on only one axial mode by introduction of pure radiation into this mode during its build-up time. Successful locking is obtained providing that the injected frequency matches only one axial mode and that the seeded power is sufficiently high compared to the noise level. Thus, the injected mode starts to deplete the pump before any adjacent mode can oscillate. Compared to spectrally selective cavities, the injection technique is very attractive since the OPO does not suffer from additional optical losses. Consequently, a low threshold of oscillation and a high conversion-efficiency are expected. The efficiency could even overcome the unseeded case due to a reduction of the build-up time of the seeded mode. However, the dynamic of a seeded OPO is not trivial and several mechanisms can lead to a frequency shift between the injected frequency and the OPO output [13,14] even if the OPO cavity length is resonant at the injected wavelength. Basically, the OPO frequency can differ from the seeded one given the following processes:

- if the parametric gain of one unseeded mode becomes higher than the gain of the seeded mode, then the mode with the higher gain will overtake the seeded mode leading to a mode hop. Such a behaviour can be seen if the seeded mode is not exactly at the peak of the parametric gain curve or at a high pumping level due to a cascading process (in a first step, the pump is completely depleted by the growth of the seeded mode, in a second step, back conversion of the signal and idler waves provides radiation available for pumping another mode);
- in case of phase mismatch, the amplified wave (signal or idler) experiences a phase shift because the wave vector of the nonlinear polarisation is not equal to that of the amplified waves. Frequency shifts of several hundreds of MHz can be observed under phase mismatch condition [14]. In pulsed operation, a frequency chirp can also be introduced given that the phase mismatch varies somewhat with the pump intensity;
- in case of a small optical feedback of the nonresonant wave, the maximum gain value depends on the relative phase  $\phi_p - (\phi_s + \phi_i)$  between the three waves and consequently the phase of the resonant mode can be shifted to maintain the gain at its maximum value. Such a situation can produce a frequency shift of several tens of MHz [13];
- nonlinear index of refraction can modified the frequency resonance of the cavity as a result of the variation of the nonlinear index of refraction (Kerr effect) induced by the pump field. This change will modify the output frequency of the OPO (over 10 MHz, typically) with regard to the injected frequency.

If we compare the performance obtained with a seeded OPO and a solution based on a dispersive cavity, it is clear that only the first method is able to provide a powerful output (several tens of mJ) given the absence of insertion optical losses and the high efficiency. However, the injection-seeding technique suffers from several drawbacks:

- the complexity, which requires delicate adjustments, high mechanical stability and optical isolation;
- the necessity to actively stabilize two optical cavities (injection and slave);
- the high sensitivity of external cavity diode-lasers to mechanical vibrations;
- the limited availability of wavelengths with diode-lasers.

### 3.2. Dual cavity doubly resonant OPOs

Historically, doubly resonant OPOs were the first to be developed because of the lower threshold requirements. However, initial experiments clearly show that these devices were highly unstable and that oscillation was impossible to achieve at particular wavelengths [15]. Much work has been done to well understand such a behaviour, see reference [16] for a theoretical analysis. It was concluded that because of crystal dispersion, the optical length of the resonator differs at the signal and idler wavelength and consequently, both wavelengths are not in general simultaneously resonant. In other words, the specifications for oscillation in doubly resonant OPOs are over constrained by requiring three specifications to be simultaneously fulfilled: the energy conservation and two resonant conditions at the signal and idler wavelengths within a single optical cavity. Therefore, doubly resonant oscillation occurs only at particular frequencies where the signal and idler frequencies are jointly in resonance with the resonator. This behaviour was called ‘cluster effect’ in doubly resonant OPOs. One solution to overcome this limitation is to use a dual-cavity architecture as shown schematically in Fig. 7. In such a way, the signal and idler cavity lengths can be controlled separately, eliminating so the over-constraint condition. Furthermore, by choosing carefully the difference in length between the two cavities, one can select only one common coincidence within the signal and idler combs, so achieving doubly resonant oscillation at only one frequency (Vernier effect). The Giordmaine and Miller’s diagram [17] shown in Fig. 8, illustrates such a mode selection: within the parametric gain curve, only the pair of signal and idler modes that are located along the same vertical line can oscillate.

A comprehensive analysis of the conditions that have to be fulfilled to achieve single-longitudinal-mode operation has been conducted in [18]. From this previous work, it was concluded that the optimal geometry requires cavity lengths as short as possible to benefit from large free spectral ranges whereas the crystal length has to be as long as possible in order to reduce the parametric gain band width as well as the threshold of oscillation. To fulfil these two contradictory conditions, we have developed a compact entangled-cavity doubly resonant optical parametric oscillator (ECOPO) [19], shown schematically in Fig. 9. The entangled cavity is composed of four mirrors symmetrically placed on each side of the crystal. The signal and idler waves oscillate between the pairs of mirrors M1–M3 and M2–M4, respectively. The inner mirrors (M1, M4) are deposited onto the crystal faces whereas the external mirrors (M2, M3) are mounted on two PZT actuators for fine tuning. The radius-of-curvature of external mirrors are chosen to optimize the mode overlapping between the two cavities and the pump beam.

The first validation experiments of this arrangement were carried out with a multi-kHz repetition rate Nd:YAG laser while the idler radiation was emitted around 4  $\mu\text{m}$  [19]. Thanks to the low threshold of oscillation of the doubly resonant configuration, the parametric oscillation was obtained in a 6 mm-long PPLN crystal with less than 10  $\mu\text{J}$  of pump energy. Fig. 10 illustrates the spectral behaviour of the ECOPO for two different cavity lengths. Although

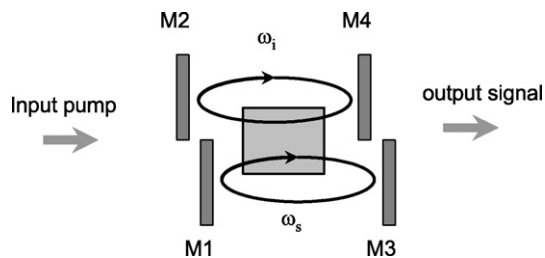


Fig. 7. Scheme of a dual-cavity doubly resonant OPO.

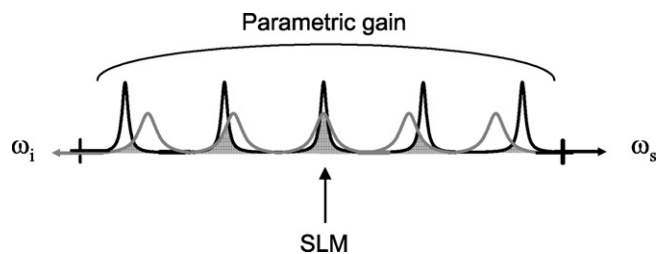


Fig. 8. Illustration of the mode selection based on the Vernier effect. Note that the signal and idler frequency axes are oriented in opposite directions to fulfil the conservation of the energy (Giordmaine and Miller representation).

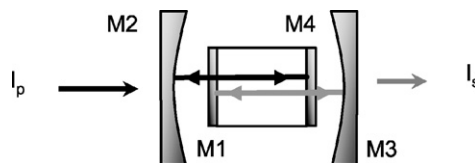


Fig. 9. Geometry of the entangled cavity doubly resonant OPO.



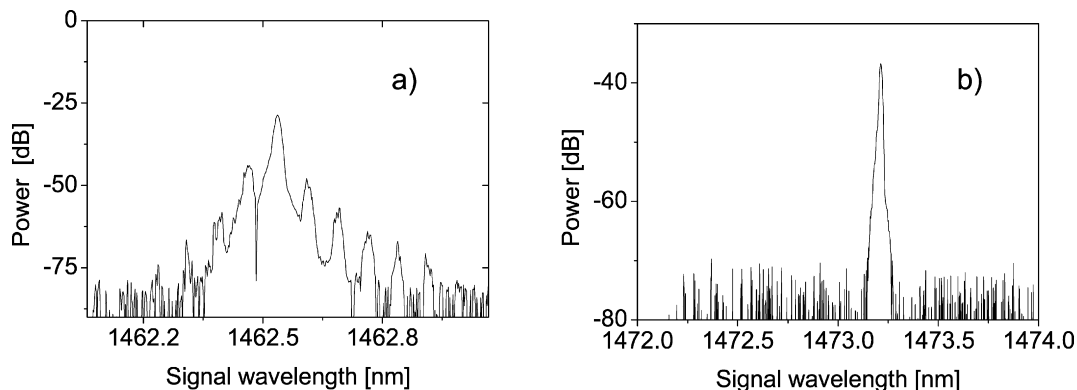


Fig. 10. Spectral output of the entangled cavity doubly resonant OPO obtained by monitoring the signal radiation with an optical spectrum analyzer; situations (a) and (b) have been obtained when the signal and idler cavity lengths differ from 3 and 7%, respectively.

adjacent modes can simultaneously oscillate if the two cavities are very close (within 3%), single longitudinal mode output is achieved if the two lengths differ from 7%; in this last case, a SMSR of more than 40 dB is achieved, demonstrating the high spectral rejection of the Vernier approach. Compared to previous methods listed in Section 3.1, the ECOPO configuration shows two major advantages:

- one obtains single longitudinal mode operation by taking advantage of the low threshold of oscillation of doubly resonant coincidences whereas other approaches (Fabry Perot étalon or Littman configurations) suffer from an increase of optical losses due to the insertion of a selective element;
- single frequency can be achieved all over the operating range of the OPO whereas it is limited to the spectral tuneability of an external source for seeded OPOs;
- very compact devices can be designed thanks to the linear geometry of the ECOPO.

On the other hand, the following limitations are encountered:

- very demanding coating specifications have to be fulfilled, given that each mirror has to be designed to filter out one specific radiation among three;
- the extracted power is limited at a low level (less than 1 mJ, typically) as a consequence of the limited pump energy that has to be applied to achieve the doubly resonant oscillation.

The coating quality is clearly a critical issue regarding the capability to control and to tune the output frequency of the ECOPO. Indeed, a small parasitic reflection at the pump wavelength on mirror M3 or M4 has a strong influence on the oscillation threshold. As illustrated in Fig. 11, only a 0.5% reflection of the pump radiation onto M3 is enough to modulate the threshold of oscillation by more than 20% depending on the relative phase value  $\Delta\phi = \phi_p - (\phi_s + \phi_i)$  that takes place between the three waves after reflection.

In order to reduce the sensitivity of the ECOPO to unwanted pump reflections, we used a two-pass pump beam scheme. Experimentally, one introduces a flat mirror M5 at the exit of the ECOPO to reflect 80% of the pump radiation, see Fig. 12. This mirror is mounted on a PZT actuator for fine adjustment of the phase  $\Delta\phi = \phi_p - (\phi_s + \phi_i)$  between the three waves travelling in the backward direction. According to Bjorkholm et al. [20], the parametric conversion can take place back and forth in the nonlinear crystal providing that  $\Delta\phi$  is adjusted to an optimal value that depends on the phase-mismatch  $\Delta k = k_p - (k_s + k_i)$  between the three interacting fields,  $k_j$  is the wave-vector of the  $j$ th field. In case of birefringence phase matching, it was demonstrated in [20] that the optimal value is  $\Delta\phi = 0$  for perfect phase matching ( $\Delta k = 0$ ). Under quasi-phase matching, the situation is slightly different given that the thickness of the last ferro-electric domain, which is crossed over by the three fields before reflection onto M5 plays a major role on the optimal value of  $\Delta\phi$ . Indeed, if the thickness of the last domain is equal to one coherence length, a phase change  $\Delta\phi = \pi$  is needed to compensate for the phase-mismatch that has been accumulated after the three beam propagation through the last domain. Still, whatever the thickness of the last ferroelectric domain, one can always

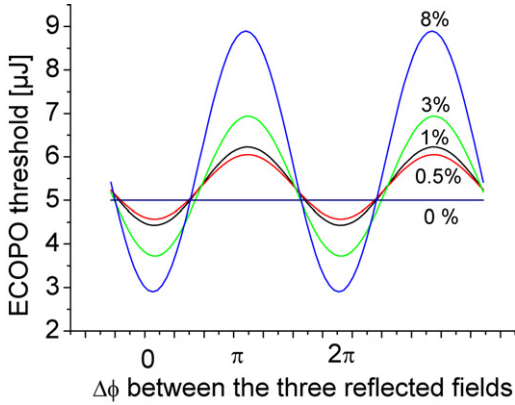


Fig. 11. Evolution of the threshold of oscillation for different values of a residual pump reflection onto M3 versus the relative phase between the three reflected fields. The calculation has been made for the ECOPO configuration depicted in Fig. 9.

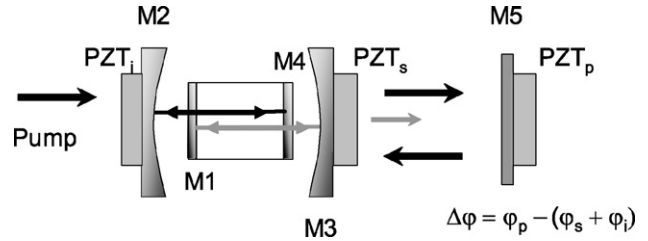


Fig. 12. Experimental arrangement of the entangled cavity doubly resonant OPO with a double pass pump beam.

find the optimal phase value by acting on the M5 PZT voltage. Hence, the quasi-phase matching condition is fulfilled in both directions leading to an effective length that is two times longer than the crystal length. The role of the M5 mirror is more quantitatively illustrated in Fig. 13 where the evolution of the idler power has been plotted versus the input pump power with and without pump reflection. The calculation has been done for a 50  $\mu\text{m}$  pump beam waist within the 6 mm long PPLN crystal, assuming that  $\Delta\phi$  has been adjusted to its optimal value so that the quasi-phase matching condition is fulfilled in both directions. It is seen that the threshold of oscillation is reduced by a factor four thanks to the 80% pump reflection. Such a decrease agrees well with the expected value given that the ECOPO efficiency is increased by a factor four as a result of the two-pass pump beam. The slope efficiency does not change significantly with and without pump reflection.

Fine frequency tuning of the ECOPO is achieved by adjusting simultaneously the three PZT voltages to maintain the mode overlap between the signal and idler cavity as well as the optimal phase value between the three fields interacting in the backward direction. One can easily derive that the drive voltages of the three PZT have to be changed according to the following relationship:

$$\frac{\Delta V_s}{\Delta V_i} = -\frac{L_s \omega_i}{L_i \omega_s} \quad \text{and} \quad \Delta V_p = f(\Delta k, \omega_p, \omega_i) \sim \frac{\omega_i}{\omega_p} \Delta V_i \quad (2)$$

where  $\Delta V_s$ ,  $\Delta V_i$  are the PZT voltages for the signal and idler cavities,  $\Delta V_p$  is the PZT voltage for the pump reflection,  $L_s$  and  $L_i$  are the signal and idler cavity lengths,  $\omega_j$  the frequency of the  $j$ th field and  $\Delta k$  the phase mismatch. Practically, the PZT are automatically driven through a Labview software. It is then possible to achieve continuous tuning over  $3 \text{ cm}^{-1}$  (limited to the maximum PZT displacement), see Fig. 14.

As predicted in Fig. 13, the two-pass pump beam ECOPO benefits from a low threshold of oscillation that allows us to use a very compact pump laser. Such a capability has been recently demonstrated by pumping the ECOPO with a commercial Nd:YAG micro-laser ( $\mu\text{Flare}$  product from Lumanova GmbH). The very compact laser head, see Fig. 15(a), delivers 6  $\mu\text{J}$ , 6 ns long pulses at a 4.35 kHz repetition rate. Only half of the laser energy was available for pumping the ECOPO given that the laser beam was randomly polarized. The ECOPO oscillation was achieved at a 2  $\mu\text{J}$  pump level. At 1.5 times above threshold, the OPO delivers 5 ns long pulses (FWHM) with an idler energy of 0.15  $\mu\text{J}$  (i.e. 30 W peak power) at 3.9  $\mu\text{m}$ . By carefully adjusting the length of both cavities, one can achieve single-longitudinal-mode output. Fig. 15(b) demonstrates that stable single-longitudinal-mode operation can be obtained over several minutes providing that at least two PZT are actively controlled in order to maintain the mode coincidence between the two cavities as well as the optimal phase value between the three reflected fields. The fine-tuning range of the ECOPO is currently limited to 7 GHz as a result of the low pump energy level. The next developments will be carried out with a linearly polarized beam to increase the available pump energy by a factor two.

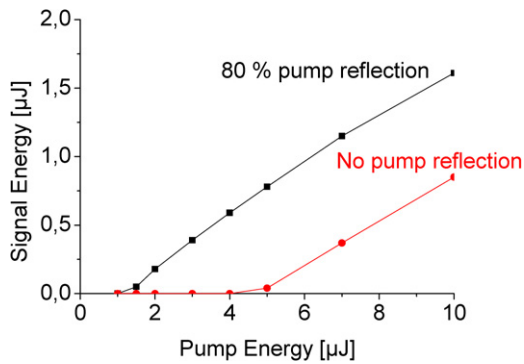


Fig. 13. Evolution of the idler energy versus the input pump energy with and without pump reflection. The position of the M5 pump mirror has been adjusted to achieve the maximum conversion efficiency.

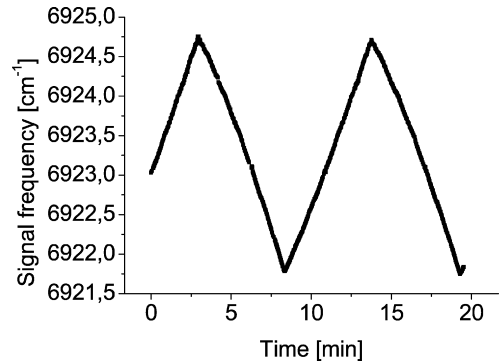


Fig. 14. Fine frequency tuning of the signal wavelength recorded by adjusting simultaneously the three PZT actuators. The frequency tuning range is limited by the PZT displacements.

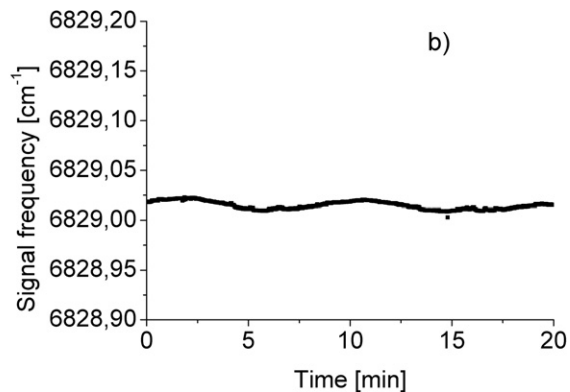
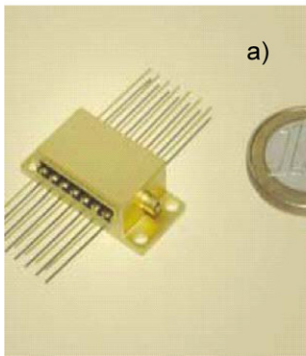


Fig. 15. (a) Microlaser head used to pump the entangled cavity doubly resonant OPO; (b) ECOPO signal frequency evolution.

#### 4. Conclusions

In this article, we have presented three different architectures that take advantage of the specific properties of the parametric conversion process. Although classical OPO devices are based on configurations where one radiation is stored within an optical cavity whereas the other one produced from the nonlinear interaction is available for the user, we have shown that specific architectures can be designed to reach new specifications. Thus, a cross-resonant OPO where a mixed oscillation is sustained within a four-mirror cavity can be well suitable to reduce the saturation effects and to increase so the optical conversion efficiency of the parametric process at high pumping levels. Besides, an OPO–OPA scheme where the idler field is used at a pump radiation in a second nonlinear interaction is an efficient method to produce a broadband radiation around  $3\ \mu\text{m}$  for applications such as laser ultrasonic inspection of composite materials. Otherwise, the oscillation at the signal and idler wavelengths can be obtained in two separate cavities so as to reduce the emitted line width and to achieve a single-longitudinal-mode emission at a very low threshold of oscillation. Such architecture is well promising to develop compact and robust laser source for gas monitoring applications.

Further improvements are expected thanks to recent developments of quasi-phase matched semiconductor materials, as well as the availability of new pump lasers. For example, the implementation of fiber lasers in parametric devices should be an interesting approach to develop efficient  $\mu\text{s}$  tuneable sources as a result of a low threshold of oscillation and a high optical conversion efficiency in the microsecond-time scale.

#### References

- [1] K. Koch, G.T. Moore, E.C. Cheung, Optical parametric oscillation with intracavity difference-frequency mixing, *J. Opt. Soc. Am. B* 12 (1995) 2268–2273.

- [2] M. Dubois, P.W. Lorraine, R.J. Filkins, T.E. Drake, Experimental comparison between optical spectroscopy and laser-ultrasound generation in polymer-matrix composites, *Appl. Phys. Lett.* (2001) 1813–1815.
- [3] D.R. Guyer, D.D. Lowenthal, Novel cavity design for a high efficiency, high energy near infrared  $\beta$ -BaB<sub>2</sub>O<sub>4</sub> parametric generator, in: *Non-linear Optics*, in: *Proc. SPIE*, vol. 1220, 1990, pp. 41–44.
- [4] A. Godard, M. Raybaut, O. Lambert, J.-P. Faléni, M. Lefebvre, E. Rosencher, Cross-resonant optical parametric oscillators: study of and application to difference-frequency generation, *J. Opt. Soc. Am. B* 22 (2005) 1966–1978.
- [5] A. Godard, E. Rosencher, Energy yield of pulsed optical parametric oscillators: a rate-equation analysis, *IEEE J. Quantum Electron.* 40 (2004) 1527–1531.
- [6] L.B. Kreuzer, Single mode oscillation of a pulsed singly resonant optical parametric oscillator, *Appl. Phys. Lett.* 15 (1969) 263–265.
- [7] G. Robertson, A. Henderson, M.H. Dunn, Efficient, Single-axial mode oscillation of a beta barium borate optical parametric oscillator pumped by an excimer laser, *Appl. Phys. Lett.* 62 (1993) 123–125.
- [8] G.W. Baxter, P. Schlup, I.T. McKinnie, J. Hellström, F. Laurell, Single-mode near-infrared optical parametric oscillator based on periodically poled KTP, *Appl. Opt.* 40 (2001) 6659–6662.
- [9] P. Schlup, G.W. Baxter, I.T. McKinnie, Single-mode near and mid-infrared periodically poled lithium niobate optical parametric oscillator, *Opt. Comm.* 176 (2000) 267–271.
- [10] W.R. Bosenberg, D.R. Guyer, Broadly tunable, single-frequency optical parametric frequency conversion system, *J. Opt. Soc. Am. B* 10 (1993) 1716–1722.
- [11] J. Mes, M. Leblans, W. Hogervorst, Single-longitudinal mode optical parametric oscillator for spectroscopic applications, *Opt. Lett.* 27 (2002) 1442–1444.
- [12] J.E. Bjorkholm, H.G. Danielmeyer, Frequency control of a pulsed optical parametric oscillator by radiation injection, *Appl. Phys. Lett.* 15 (1969) 171–173.
- [13] D.C. Hovde, J.H. Timmermans, G. Scoles, K.K. Lehman, High power injection seeded optical parametric oscillator, *Opt. Comm.* 86 (1991) 294–300.
- [14] T.D. Raymond, W.J. Alford, A.V. Smith, M.S. Bowers, Frequency shifts in injection-seeded optical parametric oscillators with phase mismatch, *Opt. Lett.* 19 (1994) 1520–1522.
- [15] J.E. Bjorkholm, Some spectral properties of doubly and singly resonant pulsed optical parametric oscillators, *Appl. Phys. Lett.* 13 (1968) 399–401.
- [16] J. Falk, Instabilities in the doubly resonant parametric oscillator: a theoretical analysis, *IEEE J. Quant. Electr.* QE-7 (1971) 230–235.
- [17] J.A. Giordmaine, R.C. Miller, Optical parametric oscillation in LiNbO<sub>3</sub>, in: P.L. Kelley, B. Lax, P.E. Tannenwald (Eds.), *Physics of Quantum Electronics*, McGraw-Hill, New York, 1966, pp. 31–42.
- [18] B. Scherrer, I. Ribet, A. Godard, E. Rosencher, M. Lefebvre, Dual-cavity doubly resonant optical parametric oscillator: demonstration of pulsed single-mode operation, *J. Opt. Soc. Am. B* 17 (2000) 1716–1729.
- [19] C. Drag, A. Desormeaux, M. Lefebvre, E. Rosencher, Entangled-cavity optical parametric oscillator for mid-infrared pulsed single-longitudinal-mode operation, *Opt. Lett.* 27 (2002) 1238–1240.
- [20] J.E. Bjorkholm, A. Ashkin, R.G. Smith, Improvement of optical parametric oscillators by non resonant pump reflexion, *IEEE J. Quant. Electron.* QE-6 (1970) 797–799.